



Respiratory Vaccination with Hemagglutinin Nanoliposomes Protects Mice from Homologous and Heterologous Strains of Influenza Virus

Zachary R. Sia,^a Kevin Chiem,^{b,c} Wei-Chiao Huang,^a Amal Seffouh,^d Amir Teimouri Dereshgi,^{e,f} Tara Hogan,^{e,f} Joaquin Ortega,^d Bruce A. Davidson,^{e,f} Luis Martinez-Sobrido,^{b,c} Jonathan F. Lovell^a

^aDepartment of Biomedical Engineering, University at Buffalo, State University of New York, Buffalo, New York, USA

^bTexas Biomedical Research Institute, San Antonio, Texas, USA

^cDepartment of Microbiology and Immunology, University of Rochester, Rochester, New York, USA

^dDepartment of Anatomy and Cell Biology, McGill University, Montreal, Quebec, Canada

^eVeterans Administration Western New York Healthcare System, Buffalo, New York, USA

^fDepartment of Anesthesiology, University at Buffalo, State University of New York, Buffalo, New York, USA

ABSTRACT Intranasal vaccination offers the potential advantage of needle-free prevention of respiratory pathogens such as influenza viruses with induction of mucosal immune responses. Optimal design of adjuvants and antigen delivery vehicles for intranasal delivery has not yet been well established. Here, we report that an adjuvant-containing nanoliposome antigen display system that converts soluble influenza hemagglutinin antigens into nanoparticles is effective for intranasal immunization. Intranasal delivery of nanoliposomes in mice delivers the particles to resident immune cells in the respiratory tract, inducing a mucosal response in the respiratory system as evidenced by nasal and lung localized IgA antibody production, while also producing systemic IgG antibodies. Intranasal vaccination with nanoliposome particles decorated with nanogram doses of hemagglutinin protected mice from homologous and heterologous H3N2 and H1N1 influenza virus challenge.

IMPORTANCE A self-assembling influenza virus vaccine platform that seamlessly converts soluble antigens into nanoparticles is demonstrated with various H1N1 and H3N2 influenza antigens to protect mice against influenza virus challenge following intranasal vaccination. Mucosal immune responses following liposome delivery to lung antigen-presenting cells are demonstrated.

KEYWORDS immunization, influenza, intranasal, liposomes, subunit vaccine

Influenza infections represent a significant disease burden in the worldwide human population. Annual vaccination against emerging strains of influenza virus helps to control and prevent epidemics. However, current methods possess drawbacks that limit their effectiveness. In the past 10 years, the overall seasonal influenza vaccine effectiveness has ranged from as low as 19% in the 2014–2015 season to a peak of 60% in 2010–2011 (1). Further compounding the challenge of preventing influenza infections are human factors involved with the vaccine, which reduces vaccine coverage in the population. In the 2020–2021 season, the coverage among adults 18 and older was only 50.2% (2). One proposed method for enhancing current vaccine practices is delivery via the intranasal route, by which a vaccine is introduced to the respiratory tract mucosal epithelium through a nasal spray solution delivered through a simple syringe adapter. The intranasal route has long been considered a promising route for influenza virus vaccination (3). A 2000 study found that of 1,600 patients who elected to receive a free vaccine of either intranasal or injectable delivery, 97% of patients preferred the intranasal vaccine (4). Several other clinical studies support the intranasal route of administration for

Editor Kanta Subbarao, The Peter Doherty Institute for Infection and Immunity

Copyright © 2022 American Society for Microbiology. All Rights Reserved.

Address correspondence to Bruce A. Davidson, bdavidso@buffalo.edu, Luis Martinez-Sobrido, lmartinez@txbiomed.org, or Jonathan F. Lovell, jflovel@buffalo.edu.

The authors declare a conflict of interest. W.-C.H. and J.F.L. hold interest in POP Biotechnologies. Other authors declare no conflict.

Received 1 July 2022

Accepted 26 August 2022

Published 15 September 2022

influenza vaccines (5–7). In addition to potentially increasing vaccine coverage, intranasal delivery may also provide unique immunological benefits. Research has shown that the mucosa-associated lymphoid tissues (MALT) compose a compartmentalized aspect of the immune system with distinct characteristics and specialized antigen-presenting cell (APC), B-cell, and T-cell populations (8). Therefore, it is theorized that activation of the MALT localized within the respiratory tract would prime these tissues against infection (8–11).

Live-attenuated influenza vaccines (LAIVs) have been approved intranasal (i.n.) vaccines for many years, with FDA-approved FluMist Quadrivalent currently on the market in the United States (12). LAIVs have a valuable role in the influenza vaccine landscape, particularly in young children, for whom inactivated vaccines are not sufficiently effective (11, 12). However, this approach has also presented unique challenges. For example, in the 2013–2014 and 2015–2016 influenza seasons, competition between attenuated virus strains resulted in decreased protective efficacy against the H1N1 component of the vaccine (13). To improve i.n. vaccines, research has turned toward adjuvanted proteins and nanoparticles as a method for targeting this route. While the (i.n.) immunization route poses many distinct challenges relative to intramuscular (i.m.) delivery (14), numerous potential candidates have arisen in prior years. One candidate has been liposomal particles, of which heat-labile toxin (HLT)-adjuvanted virosomes (15) and CAF01-adjuvanted liposomes have presented some promise (16). Here, we investigated a novel antigen-binding liposomal nanoparticle solution with the capability for i.n. delivery. It has recently been shown that other delivery systems based on emerging nanomaterials such as cationic graphene oxide can enhance i.n. vaccine responses in mice (17). To this end, we tested the use of recombinant hemagglutinin (HA) trimers displayed on cobalt-porphyrin phospholipid (CoPoP) liposomes as a nanoparticle-based vaccine for i.n. delivery. The CoPoP vaccine system converts soluble his-tagged antigens into immunogenic liposome-displayed particles and was recently demonstrated to be effective for binding and stimulating immune response against influenza HA antigen (18). These liposomes are additionally adjuvanted with a synthetic monophosphoryl lipid A (3D6A-PHAD; abbreviated as PHAD within this article) to increase the immune response to the particles. CoPoP liposomes have recently entered human clinical trials as part of a COVID-19 vaccine (NCT04783311) using a monophosphoryl lipid A produced in engineered *Escherichia coli*. In this study, we demonstrate the i.n. delivery approach utilizing CoPoP liposomes that represents a potential option for future influenza vaccine development.

RESULTS

Intranasal vaccination delivers liposomes to the lung-resident antigen-presenting cells. The biodistribution of liposomes bearing porphyrin phospholipids (PoP) was assessed in mice. Equal volumes and doses of liposomes were administered by i.m. injection of the hindleg or i.n. inoculation. PoP possesses inherent fluorescent properties enabling detection and quantification in tissues by fluorescent imaging methods (19, 20). After 24 h, mice were sacrificed, and organs were extracted for fluorescent imaging. i.m. injection resulted in liposomes primarily being visualized in the liver. In contrast, i.n. administration resulted in high concentrations of liposomes in the lung tissues, with some liposomes also deposited in the gastrointestinal (GI) tract, compared to the basal levels of GI tract epifluorescence in untreated and i.m. mice and low levels of delivery to the liver in i.m. mice (Fig. 1A). Thus, in these particular i.n. conditions, much of the vaccine was delivered to the lower respiratory tract, which is likely not a close approximation of vaccine distribution for human i.n. immunization. Lung tissues were also analyzed for PoP uptake into resident immune cells. Flow cytometric analysis revealed that PoP liposome uptake in lung-localized immune cells was significantly higher for B cells, major histocompatibility complex (MHC) class II bearing cells, and dendritic cells when liposomes were administered i.n. (Fig. 1B). Further flow cytometric analysis of DY490 fluorescently labeled trimeric H3 antigen bound to CoPoP/PHAD liposomes showed that the vaccine antigen remains associated with the CoPoP liposomes through the uptake process and is successfully introduced to local immune cells within the respiratory tract (Fig. 1C to E).

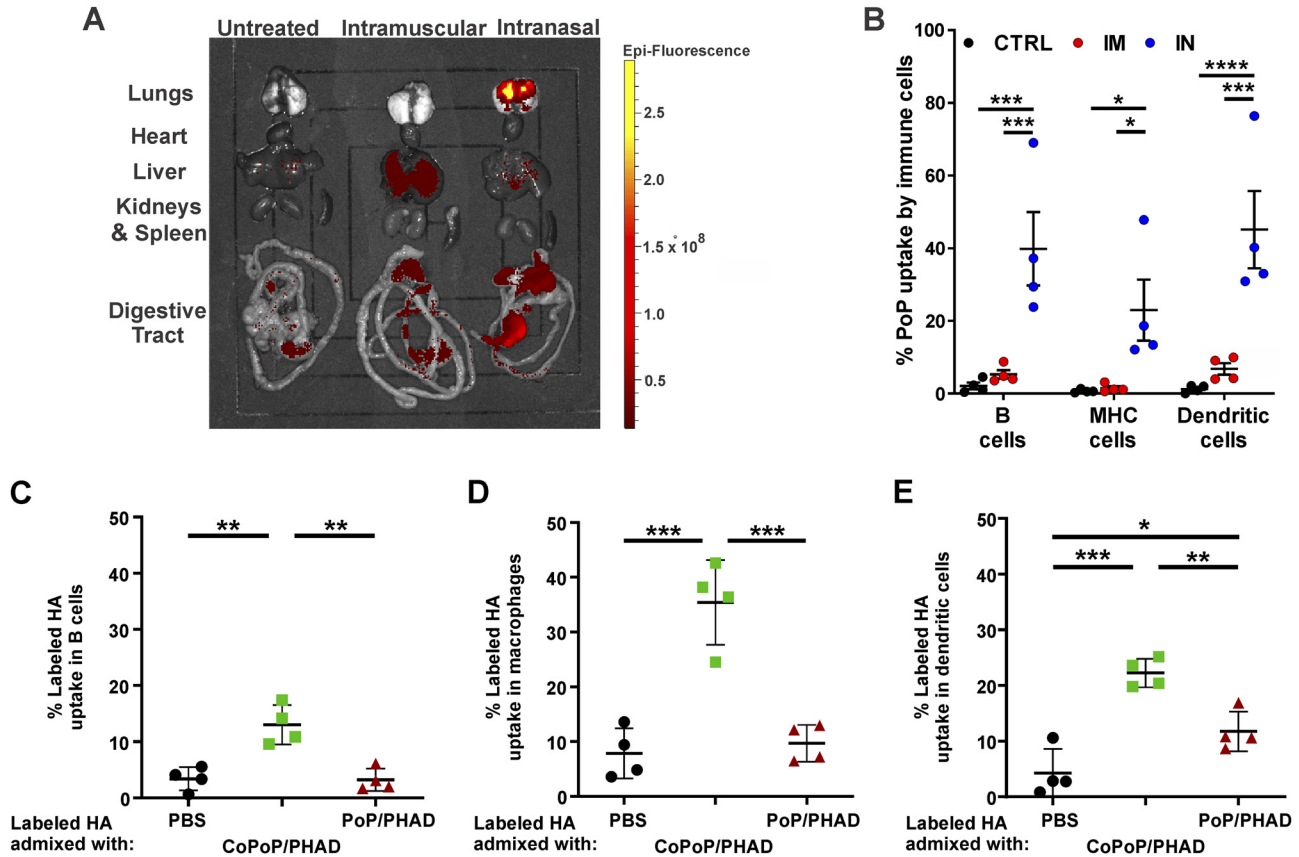


FIG 1 Intranasal (IN) administration delivers liposomes to mouse lungs better than intramuscular (IM) administration, where liposome-displayed HA is uptaken by resident immune cells. (A) Fluorescent imaging of tissues excised from mice treated with fluorescent PoP/PHAD liposomes. (B) PoP fluorescence in immune cells assessed by flow cytometric analysis of lung cell suspensions following enzymatic digestion. HA with fluorescent-labeled DY490 bound to CoPoP/PHAD liposomes show uptake into immune cells extracted from lung homogenates observed with flow cytometry. (C to E) Fluorescence at 490 nm in B cells (C), macrophages (D), and dendritic cells (E) indicates uptake of the H3 antigen. CoPoP image in panel A representative of organ samples from animals analyzed in panel B. Statistical analysis was performed in panel B by two-way ANOVA with Tukey's multiple-comparison test and in panels C to E by one-way ANOVA with Tukey's multiple-comparison test. *, $P < 0.05$; **, $P < 0.01$; ***, $P < 0.005$; and ****, $P < 0.001$. $n = 4$ mice per group.

HA antigens bind and localize on the liposomal surface. Cobalt-porphyrin phospholipids (CoPoP) readily bind histidine residues, allowing recombinant proteins with added histidine chains, a method known as his-tagging, to be anchored to the liposomal membrane surface. His-tagged influenza HA trimer antigens with trimerizing foldon domains were incubated with adjuvanted CoPoP-bearing liposomes (CoPoP/PHAD) at various ratios of HA antigen to CoPoP/PHAD liposome by mass and subjected to competition assay with nickel nitrilotriacetic acid (NTA) beads with histidine binding affinity to determine the stability of binding. Liposomes without cobalt (PoP/PHAD), which do not exhibit binding properties, were used as a negative control. It was shown that a 1:4 mass ratio of HA to CoPoP/PHAD binding was most stable, with the largest HA portion observed in the supernatant recovered from the dissolution of liposomes and negligible protein observed in the bead fraction (Fig. 2A). Analysis of the size and polydispersity of HA-CoPoP/PHAD liposomes found identical average sizes (Fig. 2B) and comparable polydispersity with nonbinding PoP/PHAD liposomes (Fig. 2C), indicating that no significant aggregation of particles occurs due to protein binding. Cryogenic transmission electron microscopy (Cryo-TEM) was used to visualize liposomes without (Fig. 2D) and with HA trimers localized to the surfaces of membranes (Fig. 2E). To visualize trimers, antigens were incubated with liposomes at a 2:1 mass ratio, as the 1:4 mass ratio utilized in vaccinations resulted in Cryo-TEM visualization that was suboptimal for antigen identification on the liposome surface.

Intranasal delivery induces mucosal antibody response. Introducing vaccines i.n. results in stimulation of the local immune system within mucus membranes, which operates in a distinct manner from the systemic immune response triggered by i.m. injection. Whereas

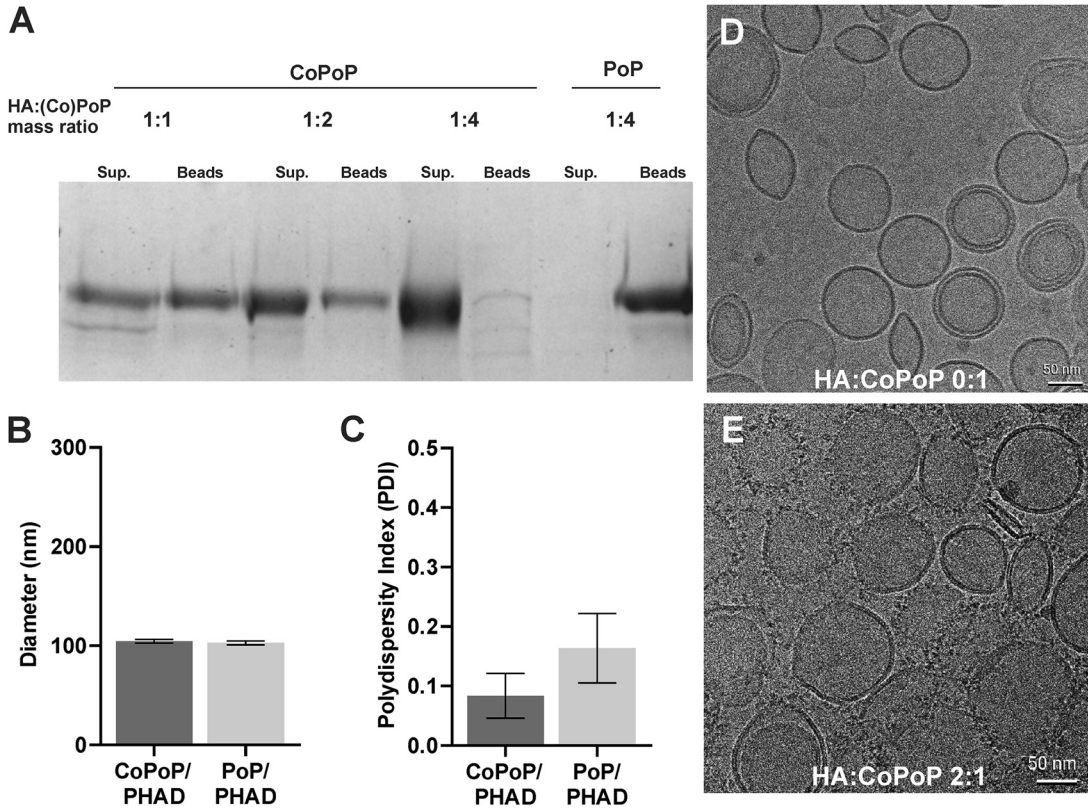


FIG 2 Liposomes effectively bind HA trimers to the membrane surface. (A) Competitive binding assay with his-tag binding CoPoP/PHAD liposomes and Nickel-NTA beads. Liposomes incubated in 1:1, 1:2, and 1:4 ratios of HA:CoPoP (HA antigen from A/Ca/Illinois/11613/2015), with nonbinding PoP/PHAD liposomes for negative control. Sup., supernatant fraction; Beads, bead fraction. (B) Average liposome size. (C) Polydispersity of liposomes. (D) TEM images of CoPoP liposomes. (E) CoPoP liposomes bound with influenza virus HA antigen at 2:1 mass ratio. Error bars in panels B and C indicate standard deviation.

systemic immunity is characterized primarily by IgG antibody production and circulation as a component of blood plasma, mucosal immunity results in the production of secreted antibodies, including IgA. Unlike IgG antibodies, the majority of which remain circulated internally within the blood serum, these antibodies are secreted to the epithelial surface of the mucous membranes, which aid in the protection of mucosal tissues by binding to antigens at the external membrane, where influenza viral uptake and infection first occur. To assess the immune response localized to respiratory tissues, mice were treated with HA-CoPoP/PHAD through i.n. or i.m. routes. Mice were then euthanized, and blood serum, nasal lavage fluid, and lung homogenates were assessed to quantify IgA and IgG present. i.n.-vaccinated animals yielded significantly higher IgA titers in all tissue samples, showing increased levels systemically in blood serum (Fig. 3A) as well as at local sites in the nasal passages (Fig. 3B) and lungs (Fig. 3C). In contrast, i.m. vaccination generally produced higher levels of IgG in serum (Fig. 3D), nasal lavage (Fig. 3E), and lung homogenates (Fig. 3F). Quantification of anti-histidine tag antibodies in all samples yielded no significant anti-his response in IgG antibodies (Fig. S2 in the supplemental material). While both methods elicited detectable IgG responses, only i.n. vaccination resulted in significant IgA production within respiratory tissues.

Intranasal vaccination protects mice in homologous challenge. i.n. CoPoP vaccination was tested against influenza viral challenge in mice to determine protective efficacy. Mice were treated with CoPoP/PHAD liposomes bound with HA from the influenza strain A/Ca/Illinois/11613/2015 (H3N2) following a 14-day prime-boost schedule with 100-ng antigen doses. Antigens from this nonhuman strain were originally selected as having high homology with the commonly used mouse-adapted A/Hong Kong/1/1968 H3N2 strain (18). Condition groups compared HA-CoPoP/PHAD to formulations without the liposomes and liposomes without PHAD adjuvant, and without cobalt to facilitate binding. HA-CoPoP/PHAD was also

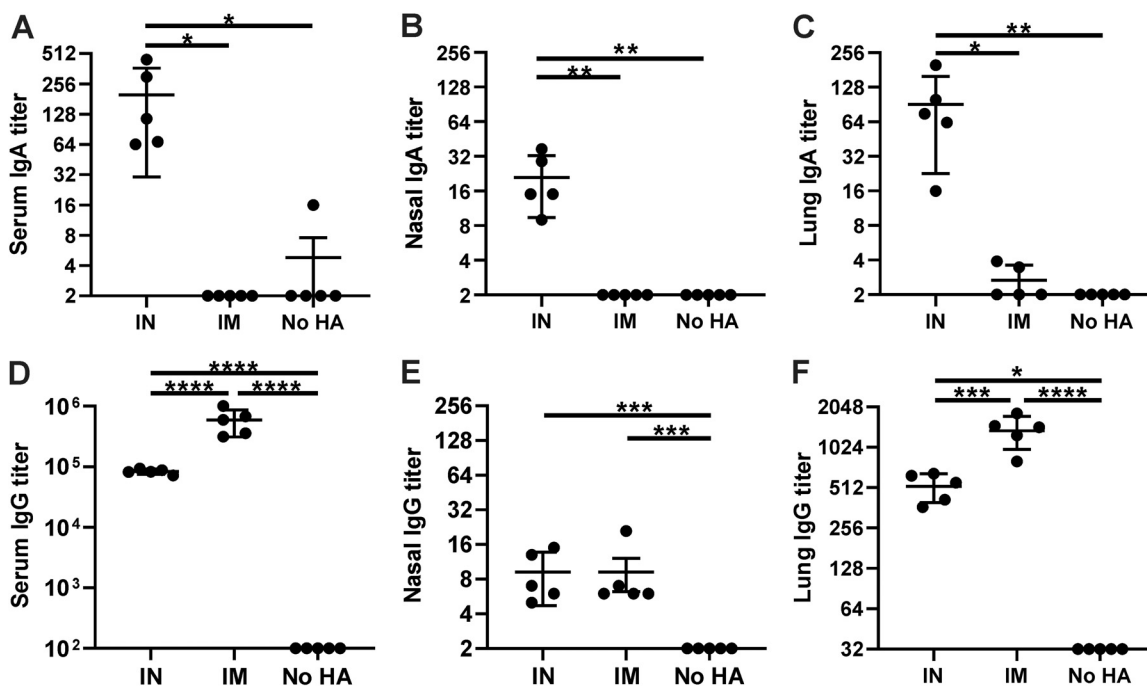


FIG 3 Intranasal administration of HA-CoPoP/PHAD induces IgA and IgG in the respiratory tract. Mice were vaccinated with 100 ng of HA trimers from A/Ca/Illinois/11613/2015 H3N2 bound to CoPoP/PHAD liposomes via the indicated route (IN, intranasal; IM, intramuscular; No HA, untreated). Following primary vaccination on day 0 and booster vaccination on day 14, serum, nasal lavage, and lung tissue were collected. IgA antibody titers measured in blood serum, nasal lavage fluid, and homogenized lung tissues (A to C) were compared against IgG antibody titers in the same tissues (D to F). Error bars indicate standard deviation. Statistical analysis was performed with one-way ANOVA with Tukey's multiple comparisons. *, $P < 0.05$; **, $P < 0.01$; ***, $P < 0.005$; and ****, $P < 0.001$.

compared against the liposomes without an antigen and antigens with an AS01-like comparative lipid adjuvant. Each of these groups was tested with both i.n. and i.m. delivery methods and further compared against typical inactivated influenza virus (IIV) vaccine and mock-vaccinated control (phosphate-buffered saline [PBS]) mice. At 14 days following the booster vaccination, mice were intranasally infected with 10^5 focus-forming units (FFU) per mouse of A/Ca/Illinois/41915/2015 influenza virus. Blood serum samples that were acquired immediately before booster vaccination and viral challenge indicated that HA-CoPoP/PHAD and HA-[AS01-like] formulations were more effective than IIV at inducing IgG antibody production when delivered i.m., but only HA-CoPoP/PHAD produced any detectable response when delivered i.n. (Fig. 4A). These prechallenge IgG levels seem to correlate with the effective protection, where HA-CoPoP/PHAD i.n., HA-CoPoP/PHAD i.m., and HA-AS01-like i.m. reduced viral load at 2 days postinfection as measured by focus-forming units (FFU). In contrast, IIV vaccine and nonbinding HA-PoP/PHAD only achieved complete reduction after 4 days of infection (Fig. 4B). Although the IgG titer elicited by HA-CoPoP/PHAD i.n. can be considered comparable to levels from HA-CoPoP and IIV vaccination, viral load was substantially reduced by day 2 postinfection, indicating that i.n. protection results from factors other than serum IgG antibody production alone. This may be attributed to the capability of HA-CoPoP/PHAD to elicit IgG within nasal mucosa, although the disparity in serum IgG suggests additional factors that provide an advantage over similarly performing AS01-like adjuvanted vaccine and IIV, such as the contribution of IgA secretory antibodies, as well as the potential for local and systemic cellular responses. For this challenge, body weight loss and survival were not measured, as prior challenges with A/Ca/Illinois/41915/2015 influenza virus in mice have been shown not to result in significant weight loss or mortality as consequences of infection with this virus (21).

Intranasal vaccination confers heterologous protection. HA-CoPoP/PHAD was assessed to determine if i.n. vaccination could contribute to protection against heterologous strains of influenza virus. Mice were vaccinated HA-CoPoP/PHAD utilizing HA antigen from A/Ca/Illinois/11613/2015 (H3N2) following a prime-boost schedule as previously described

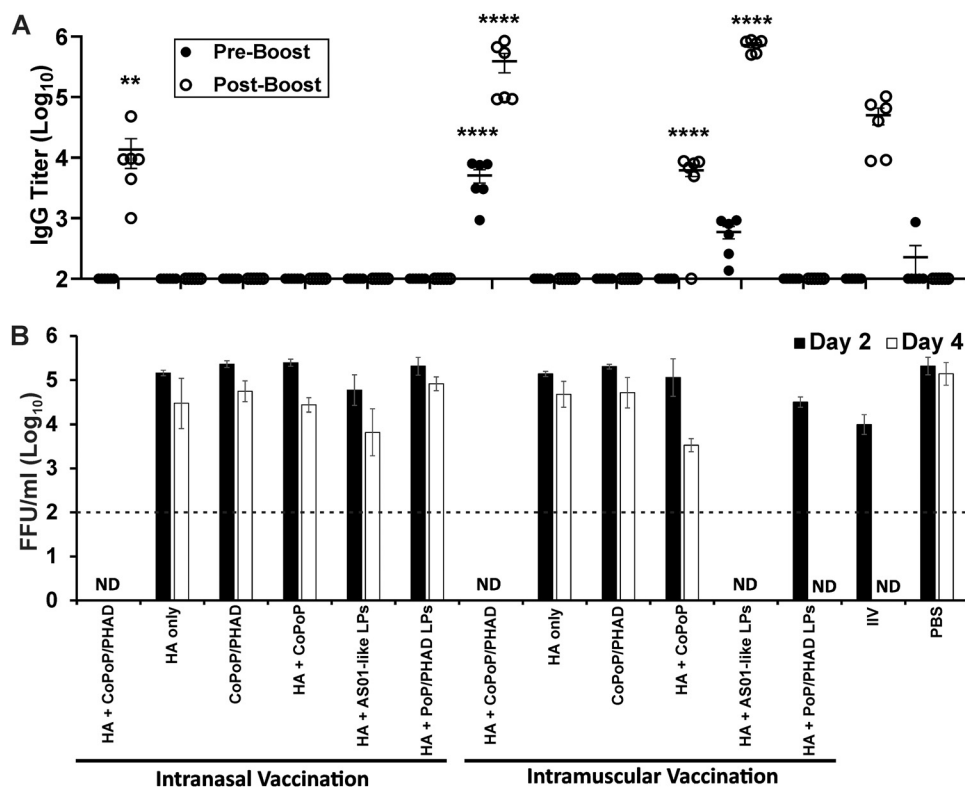


FIG 4 Intranasal administration confers protection from homologous viral challenge. Mice were vaccinated with 100 ng of HA trimers from A/Ca/Illinois/11613/2015 H3N2 admixed with indicated adjuvants. Following primary vaccination on day 0 and booster vaccination on day 14, mice were then challenged on day 28 with 10^5 FFU/mice of A/Ca/Illinois/41915/2015 H3N2. (A) IgG antibody titers in serum prior to viral challenge, compared between samples acquired after primary injection and after secondary booster injection. (B) Virus particle titers in the lungs of mice 2 days or 4 days postchallenge with A/Ca/Illinois/41915/2015 H3N2. Statistical analysis of IgG titers performed with one-way ANOVA and Tukey post test comparing all groups to the IIV-positive control. Error bars indicate standard deviation. ND, not detected. Dotted line indicates the limit of detection of the assay (100 FFU/ml). LPs, liposomes. **, $P < 0.01$; and ****, $P < 0.001$.

and then exposed to viable mouse-adapted influenza virus strain A/Hong Kong/1/1968 (H3N2) at an inoculum dose of $10 \times LD_{50}$ (400 PFU). The heterologous strain possesses a protein sequence homology of 92.50% with the antigenic strain (Table S1). The A/Ca/Illinois/11613/2015 (H3N2) antigenic strain was selected from among available strains for its relatively high antigenic matching with mouse-adapted A/Hong Kong/1/1968 (H3N2), while providing an antigenic drift, which could reflect antigenic changes over the course of seasonal epidemics, which could affect vaccine efficacy (22). For this challenge, mice were vaccinated with 100-ng antigen doses and observed for a 14-day time course to examine the overall effect of vaccination on morbidity, mortality, and recovery from influenza infection. Immediately before challenge, both i.n. and i.m. vaccination yielded significant IgG titers in sera (Fig. S1A). Although only i.m. vaccination was able to reduce the lung viral load after 4 days (Fig. 5A), both i.n. and i.m. significantly reduced body weight loss (Fig. 5B) and clinical scoring of infection symptoms (Fig. 5C) by the day 4 time point. In addition, mice vaccinated with an HA-CoPoP/PHAD solution by either route achieved survival rates of a significant margin over unvaccinated mice, and i.n. and i.m. vaccination routes were not statistically significantly different from each other (Fig. 5D). While i.n. vaccination protection does not equate to i.m. vaccination protection at this stage, i.n. vaccination has a proven capacity to meet protective benchmarks, which supports further investigation into this application for the recombinant antigen with an adjuvant system.

Mice were vaccinated with HA-CoPoP/PHAD utilizing HA antigen from A/Hawaii/70/2019pdm (H1N1) or A/California/04/2009pdm (H1N1) following a prime-boost schedule of primary vaccination on day 0 and a booster on day 21. Mice were then intranasally infected

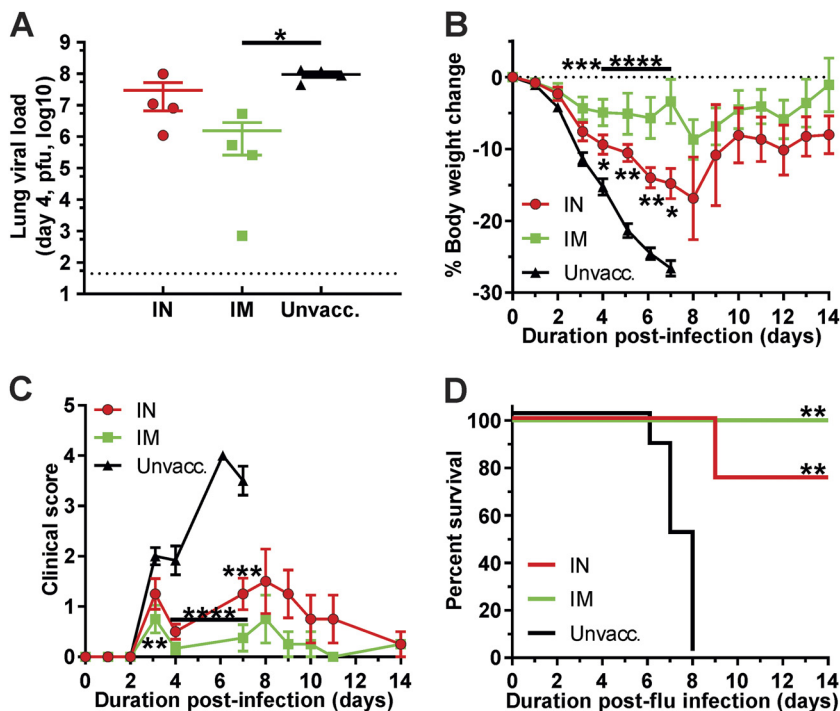


FIG 5 Intranasal administration of HA-CoPoP confers protection from H3N2 heterologous viral challenge in mice. Mice were vaccinated with 100 ng HA from A/Ca/Illinois/11613/2015 (H3N2) via intranasal (IN) or intramuscular (IM) route or were not immunized at all (black). Following primary vaccination on day 0 and booster vaccination on day 21, mice were then challenged on day 28 with $10 \times LD_{50}$ A/Hong Kong/1/1968 (H3N2) on day 42. (A) A subgroup of mice was sacrificed on day 4 to observe viral load in lung tissues by plaque assay. (B to D) Change in body weight over the 14-day challenge period (B), qualitative clinical score based on observed symptoms (C), and survival of infected mice (D) (significance relative to control, not significant difference between experimental groups). Error bars indicate standard deviation. Statistical analysis of panel A was performed with one-way ANOVA with Tukey's multiple comparisons and for panels B and C was performed with one-way ANOVA with Dunnett's multiple comparisons. Statistical analysis of panel D by log-rank Mantel-Cox test. *, $P < 0.05$; **, $P < 0.01$; ***, $P < 0.005$; and ****, $P < 0.001$.

with $10 \times LD_{50}$ (348 PFU) of mouse-adapted influenza A/California/04/2009pdm (H1N1) on day 42. These strains possess a greater protein sequence homology than the H3N2 strains (94.66%) (Table S1) but represent a 10-year period of antigenic drift. As in the prior homologous challenge, mice were vaccinated with 100 ng antigen doses and observed for a 14-day time course. Assessment of IgG titers before challenge indicated that each experimental group except i.n. delivered A/Hawaii/70/2019pdm achieved significant serum IgG titers relative to the control group (Fig. S1B). After 14 days, vaccinated mice indicated body weight recovery from the infection, while all unvaccinated mice exceeded the 25% body weight loss threshold and were sacrificed. Body weight protection was greatest among mice vaccinated with HA from A/California/04/2009pdm via i.m., followed by A/California/04/2009pdm via i.n. administration and heterologous A/Hawaii/70/2019pdm i.m., with A/Hawaii/70/2019pdm delivered i.n. being the least protective (Fig. 6A). These results are reflected in clinical score observations from days 1 through 8. However, after this time point, clinical score trends cannot be distinguished between A/California/04/2009pdm i.n. vaccination and the A/Hawaii/70/2019pdm vaccine groups (Fig. 6B). Among all vaccinated groups, only one animal in the heterologous A/Hawaii/70/2019pdm group vaccinated intranasally succumbed to illness (Fig. 6C). Although there is some degree of protection gap between i.m. and i.n. vaccination groups when administering in equal doses, all vaccines could provide significant survival over the unvaccinated control group.

DISCUSSION

While i.n. vaccines utilizing live-attenuated influenza have been available on the market for many years, there are no approved recombinant or adjuvanted influenza vaccines for i.n.

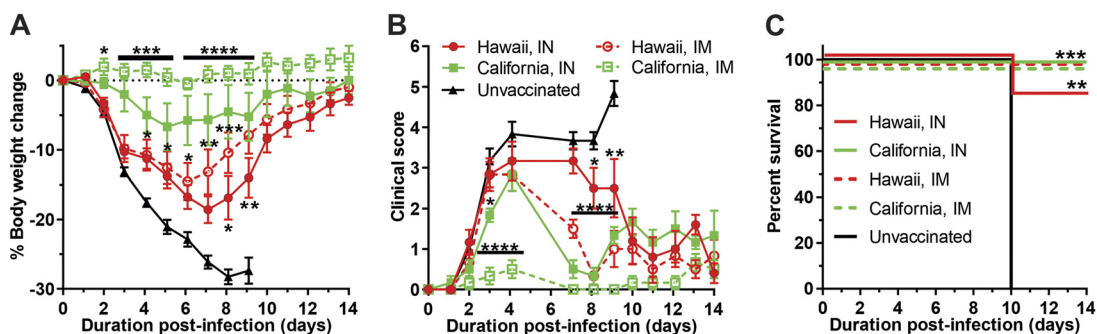


FIG 6 Intranasal administration confers protection from H1N1 homologous and heterologous viral challenge. Mice were vaccinated with 100 ng HA from either A/California/04/2009pdm (H1N1) or A/Hawaii/70/2019pdm (H1N1). Following primary vaccination on day 0 and booster vaccination on day 21, mice were then challenged with $10 \times LD_{50}$ A/California/04/2009pdm (H1N1) on day 42. Change in body weight over the 14-day challenge period (A), qualitative clinical score based on observed symptoms (B), and survival of infected mice (C). Error bars indicate standard deviation. Statistical analysis of panels A and B was performed with one-way ANOVA with Dunnett's multiple comparisons. Statistical analysis of panel C by log-rank Mantel-Cox test. *, $P < 0.05$; **, $P < 0.01$; ***, $P < 0.005$; and ****, $P < 0.001$.

delivery. While many candidates for next-generation influenza vaccines exist, many remain focused on i.m. delivery and do not consider alternative delivery routes. The research presented here represents a promising avenue for CoPoP/PHAD-based vaccines, which could combine the benefits of adjuvanted recombinant vaccines with the advantages inherent to i.n. delivery. While human i.n. vaccination would ideally be focused on the upper respiratory tract, the relatively high ratio of vaccine volume to airway volume and the short respiratory tract in the murine model resulted in a greater delivery of vaccine to the lungs. While in the murine model viral replication is predominantly localized to the lungs, which renders lung-localized delivery effective, further research is needed to determine the efficacy of delivery to the upper airways. CoPoP/PHAD liposomes localized to the respiratory tract epithelium when introduced through the nasal turbinates and reside within the tissues for 24 h to stimulate a protective immune response. Antigen-bound particles effectively elicit significant IgA secretion from the mucus membranes of the nose and lungs, which typical i.m. vaccination fails to achieve (10). The response within the respiratory tract is effective at preventing homologous-strain influenza infection, even where serological IgG titers would not suggest a sufficient response for complete protection. Against a mismatched heterologous influenza strain, i.n. vaccination significantly improved protection against severe symptoms and recovery from the disease. The research presented here supports the further investigation of the CoPoP/PHAD nanoparticle vehicle and adjuvant for influenza vaccines with i.n. delivery.

One limitation of the current research is that the cellular response was not investigated in this study. The contribution of cell-mediated immunity (CMI) plays a significant role in the mucosal immune response and protection against both homologous and heterologous influenza viral challenges. While some cursory cellular analysis of specific lung-resident immune cells has been performed here (Fig. 1B), the induction of cell-mediated response should be thoroughly characterized in a prospective human i.n. vaccine, in particular CD4 and CD8 T-cell responses. For this study, challenge results have been used to examine the sum contributions of CMI and humoral immunity in protection. Further studies with CoPoP liposomes may be optimized further with additional supporting adjuvants. Ongoing research shows that PHAD may be supplemented with immunostimulants such as trehalose-6,6-dibehenate (TDB) (16) or QS21 (23) that have been proven to enhance CMI. However, the reformulation with additional adjuvants may introduce additional complexities, especially for the i.n. route. Other adjuvants, such as AS03 and MF59, have been associated with various adverse reactions, including pain and inflammation, which could be more severe in sensitive mucous membranes (24). Some viscous adjuvants are not physically suitable for the i.n. route. Furthermore, unique adverse reactions have been linked specifically to i.n. vaccines, a notable example being cases of Bell's Palsy resulting from an IIV adjuvanted with *E. coli* heat-labile toxin (25). It may be challenging to accurately determine all the potential risks associated with i.n. administration of CoPoP/PHAD nanoparticles leading

towards clinical testing. Despite these concerns, we believe that liposomal i.n. vaccines provide a potential alternative to LAIVs, which themselves possess a history of adverse reactions or insufficient efficacy in human applications (13, 24, 25). In the case of synthetic liposomes, complexities and risks associated with the inclusion of whole or partial naturally derived virus particles may be overcome by providing greater control over particle composition.

The methodology employed for i.n. delivery in mice for these experiments is not an ideal model for i.n. vaccination in humans. Vaccines delivered by the nasal route in humans are often introduced through an aerosolized spray; however, due to the small opening of the nares in mice and shorter nasal passages, replicating this method in animal models was deemed impractical for this proof-of-principle study. Instead, vaccines were delivered dropwise by pipette to mice transiently anesthetized with isoflurane, which resulted in potentially confounding factors. First, mice were observed at times to swallow or expel vaccine fluid, which reduced the effective dose delivered to the lungs. Additional variables in the formulation and delivery of the vaccine, which can only be speculated at this time, may have also affected the resulting immunity. One such delivery variable includes vaccine dose; it has been found that reducing the volume of nasal inoculate from 50 μ l (equal to i.m. vaccine doses) to a lower volume such as 5 μ l could result in greater nasal passage localized delivery of particles, even in the murine model (26). Observing the antibody titers before challenge, IgA titers vary over a wide range (Fig. 3A to C), which likely was reflected in variable protective efficacy and a lower average body weight. Second, isoflurane has an immunosuppressive effect, which may have further reduced intranasal vaccine efficacy (27). To mitigate the effect on the results, both i.n. and i.m. groups were anesthetized before vaccination. Finally, uncertainties involving dose scaling and the possible effects of differences in upper respiratory vaccination compared to the results elicited by vaccine reaching the lungs in mice must be resolved, possibly through the application of CoPoP-based vaccines in alternative model organisms, such as ferrets.

While CoPoP particle-based vaccination delivered through the i.n. route showed lower efficacy than traditional i.m. delivery, it should be reiterated that CoPoP-based particles remain a novel vaccine nanoparticle and that the observed protection in challenge is indeed significant against both homologous and heterologous strains, warranting further study. CoPoP liposomes have shown promise for the induction of functional antibodies in a number of settings (28–33); however, this is the first study of their use for i.n. administration. Research among other i.n. vaccine formulations indicates that mucosal vaccination may also facilitate heterologous and even heterosubtypic influenza strain protection. Cross-protection has been observed resulting from the activation of CD4 and CD8 T-cells and IgA antibodies (10). Furthermore, heterosubtypic immunity has been elicited with adjuvanted i.n. vaccination using antigens from inactivated H1N1 influenza (34). Intranasal delivery has also been shown to be viable with less immunodominant, more conserved antigenic targets such as the extracellular domain of the matrix protein 2 (M2e) (35). By further optimizing particle composition and dosage parameters, we hope to attain a particle-based intranasal vaccine that exceeds the current standard set by LAIVs. i.n.-delivered particles may eventually become a delivery method of choice for future influenza vaccines, which should achieve universal protection against present and emergent strains of the influenza virus.

MATERIALS AND METHODS

Antigens. Full-length, recombinant C-terminus his-tagged HA proteins with fibrin trimerization domains for influenza virus strain A/Ca/Illinois/11316/2015 (H3N2 H3, IRR cat. no. FR1478), and A/California/04/2009pdm (H1N1 H1, IRR cat. no. FR180) were acquired from International Reagent Resource (IRR; Influenza Division, WHO Collaborating Center for Surveillance, Epidemiology and Control of Influenza, Centers for Disease Control and Prevention, Atlanta, GA, USA). Recombinant H1 HA for influenza strain A/Hawaii/70/2019 (H1N1), residues 18–530, was produced by Kinnakeet Biotechnology in Sf9 insect cells using a baculovirus system, and had a N-terminal gp67 leader sequence and a C-terminal fibrin trimerization domain followed by a hexahistidine tag, and was purified with standard immobilized metal chromatography followed by gel filtration purification on a Superdex 200 SEC column.

Cells and viruses. Madin-Darby canine kidney cells (MDCK; ATCC CCL-34) were grown and maintained in Dulbecco's modified Eagle's media (DMEM; Corning) supplemented with 10% fetal bovine serum (FBS), 1% PSG (100 units/ml penicillin, 100 μ g/ml streptomycin, and 2 mM L-glutamine) at 37°C, and 5% CO₂. Influenza A/Ca/Illinois/41915/2015 (H3N2) was obtained from the Baker Institute for Animal Health at Cornell University.

Mouse-adapted influenza A/California/04/2009pdm (H1N1) was a generous gift from Richard J. Webby of Saint Jude Children's Research Hospital (Memphis, TN). Viral infections of tissue cell culture were done by diluting A/Ca/Illinois/41915/2015 (H3N2) in phosphate-buffered saline (PBS) containing 0.3% bovine albumin (BA) and 1% PS (penicillin and streptomycin). After viral adsorption for 1 h at room temperature, inoculum was removed and MDCK cells were maintained in postinfection media DMEM with 0.3% BA, 1% PSG, and 1 $\mu\text{g/ml}$ *N*-tosyl-L-phenylalanine chloromethyl ketone (TPCK)-treated trypsin (Sigma). Viral titers in the tissue culture supernatants collected at 48 h postinfection were determined by immunofocus assay (FFU/ml) in MDCK cells. Briefly, confluent monolayers of MDCK cells (96-well plate format, 5×10^4 cells/well, triplicates) were infected with 10-fold dilutions of tissue culture supernatants at 33°C. Then, 12 h postinfection, the cells were washed with PBS, and individual infected cells were detected using the monoclonal antibody HT-103 against the viral nucleoprotein (NP) and were visualized using a fluorescence microscope to determine FFU/ml. The canine influenza A/Ca/IL/12191/2015 (H3N2)-inactivated vaccine (IV) was obtained from Zoetis (Parsippany-Troy Hills, NJ).

Liposome preparation. CoPoP was synthesized as previously described (19), and CoPoP/PHAD liposomes were prepared by ethanol injection and nitrogen-pressurized lipid extrusion. The composition of the liposomes included 1,2-dioleoyl-sn-glycero-3-phosphocholine (DOPC), cholesterol (PhytoChol; Wilshire Technologies), and synthetic monophosphoryl lipid A monophosphoryl hexa-acyl lipid A, 3-deacyl (3D6A-PHAD; Avanti; cat. no. 699855P). For brevity, 3D6A-PHAD is abbreviated as "PHAD" within this article. Lipids were dissolved in 1 ml of 60°C ethanol for 10 min, followed by the addition of 4 ml of 60°C phosphate-buffered saline (PBS) for another 10 min at 60°C. Liposomes were then passed through 200-, 100-, and 80-nm stacked polycarbonate filters in a lipid extruder (Northern Lipids) with nitrogen pressure. After extrusion, liposomes were dialyzed with PBS to remove ethanol. The final liposome concentration was adjusted to 320 $\mu\text{g/ml}$ CoPoP and passed through a 0.2- μm sterile filter. Liposome stock was stored at 4°C. The CoPoP/PHAD liposome formulation had a mass ratio of [DOPC:CHOL:PHAD:CoPoP] [20:5:1:1]. PoP/PHAD liposomes were made in the same way but used cobalt-free PoP instead of CoPoP. AS01-like liposomes were made in a similar manner but had a composition of [DOPC:CHOL:PHAD:QS21] [20:5:1:1]. QS21 was obtained from Desert King.

Antigen binding characterization. Nickel nitrilotriacetic acid (Ni-NTA) bead competition binding assay was performed by first incubating his-tagged HA antigens with CoPoP/PHAD for 3 h. Following this incubation period, Ni-NTA beads were washed three times with PBS and separated using a magnetic separator bar. A 25- μl volume of the HA-CoPoP/PHAD liposome solution was then introduced to the beads and incubated together for 30 min, with pipetting to resuspend the beads every 10 min. Beads were separated from the solution with the magnetic bar, and the supernatant was realiquoted. Beads were resuspended in 25 μl PBS by pipetting. A dye buffer solution was generated by mixing two parts NuPAGE LDS sample buffer (4 \times) and one part NuPAGE sample reducing agent (10 \times). Dye buffer solution was applied in a 1:3 ratio of dye to sample by volume and incubated together at 100°C for 10 min. Beads were then separated from solution by magnetic bar and realiquot, generating the bead fraction. Samples were applied to a NuPAGE 4 to 12% Bis-Tris gel (Invitrogen, by Thermo Fisher Scientific; cat. no. NP0321BOX), alongside a protein molecular weight ladder (14 to 120 kDa; Rockland Inc., Limerick, PA). The gel was run at a voltage of 200 V for 45 min, and then the gel was washed twice using water and heating with a consumer microwave oven for 10 s at high power. A staining solution was generated by combining one part ethanol with nine parts ProtoBlue Safe Colloidal Coomassie G-250 stain (National Diagnostics, Atlanta, GA) by volume. Gels were immersed in the staining solution overnight with constant shaking provided by a shake table, followed by immersion in tap water to destain overnight under the same shaking conditions. Gels were then imaged using a GelDoc Go Imaging System (Bio-Rad Laboratory Inc.).

Nanoparticle distribution imaging. Mice were treated with 500 ng CoPoP/PHAD liposomes in 50- μl doses via either intramuscular or intranasal route. Intramuscular vaccinations were performed via injection to the left quadriceps; intranasal vaccinations were performed by applying droplets of the solution via a 20- μl pipette to the nares, alternating nostrils with each drop. At 24 h after treatment, mice were sacrificed, and organs were removed. The excised organs were imaged for fluorescence with a IVIS Lumina II Imaging System.

Flow cytometry. Mice were treated with PoP/PHAD liposomes in 50- μl (500 ng PoP) doses via either intramuscular or intranasal route. At 24 h following vaccination mice were sacrificed, and lungs were collected. Lung tissue was dissociated, and cells were separated through a membrane. Cells were fixed with 4% paraformaldehyde at room temperature for 15 min protected from light, then washed three times with PBS under centrifugation at 500 rcf for 5 min, and then stained with antibodies against B220 (B-cell marker, Biolegend cat. no. 103211), IA/IE (major histocompatibility complex II marker, Biolegend cat. no. 107607), F4/80 (macrophage marker, Biolegend cat. no. 123109), or CD11c (dendritic cell marker, Biolegend cat. no. 117309) before flow cytometry. For labeling, H3 HA antigen from A/Ca/Illinois/11613/2015 was conjugated with the fluorescent label DY490 (DY-490-NHS-Ester; Dyomics; no. 490-01) by first dialyzing the antigen into 100 mM sodium bicarbonate buffer (pH 9) before labeling at a 5:1 molar ratio of protein to dye, and then subsequent dialysis back into PBS to remove unbound dye as recently described (36). The resultant HA-DY490 conjugates were bound to CoPoP/PHAD liposomes or admixed with PBS or nonbinding PoP/PHAD liposomes, which were used to immunize four mice per group. Flow cytometry studies were carried out using a BD LSRFortessa X-20 flow cytometer, and FlowJo (version 10) software was used for data analysis.

Vaccine administration. Mice were vaccinated by either i.m. or i.n. route. Mice vaccinated i.m. were injected with CoPoP/PHAD liposomes (400 ng CoPoP, 400 ng PHAD, or equivalent for controls) admixed with 100 ng HA in 50 μl of sterile PBS via the left hind leg. Mice vaccinated i.n. were anesthetized with 2.5% isoflurane in oxygen and 50 μl of vaccine was applied dropwise by pipette to the nares as described above.

Homologous influenza challenge. For mouse immunization and homologous influenza challenge experiment, 6- to 8-week-old female C57BL/6 mice ($n = 3$) were i.n. or i.m. vaccinated with the indicated conditions above, either with or without 100 ng of hemagglutinin (HA; A/Ca/Illinois/11613/2015 H3N2), admixed with

CoPoP/PHAD or PoP/PHAD liposomes. AS01-like liposomes were included as a vaccine adjuvant control. Mice were also mock-vaccinated (PBS) or vaccinated with 100 μ l/mice of commercial CIV H3N2 inactivated influenza vaccine (IV; Zoetis) as negative and positive controls, respectively. Mice were boosted 2 weeks postprime immunization. After 28 days postprime, mice were anesthetized intraperitoneally with 2,2,2 tribromoethanol (Avertin; 240 mg/kg of body weight) and challenged with 10^5 FFU/mouse of A/Ca/llinois/41915/2015 (H3N2). Morbidity was monitored daily by assessing changes in body weight after viral challenge. Mice losing more than 25% of initial body weight were considered to have reached their experimental endpoint and were humanely euthanized. At 2 and 4 days postchallenge, the lungs were extracted and homogenized. Viral titers were determined from lung homogenates by immunofocus assay (FFU/ml) in MDCK cells (96-well plates, 5×10^4 cells/well, triplicates) using 10-fold serial dilutions of homogenates. After 12 h postinfection, the cells were fixed and permeabilized in PBS containing 4% formaldehyde and 0.5% Triton X-100 for 10 min at room temperature. Then, cells were stained with a primary anti-NP MAb (HT103) for 1 h. After three washes with PBS, cells were incubated with a secondary anti-mouse FITC-conjugated antibody (Dako; 1:200) for 1 h. Infected cells were counted under a fluorescence microscope to determine virus titer. The mean titer and statistical analysis were determined using Microsoft Excel.

Heterologous influenza challenge. For the heterologous H3N2 experiment, groups of 12 female BALB/c mice from Charles River (Wilmington, MA) were vaccinated, i.n. or i.m., as described above, with 50 μ l of CoPoP/PHAD containing 100 ng his-tagged H3HA from A/Ca/llinois/11615/2015 (H3N2) with trimerization domain on day 0 and day 21. On day 42, these mice and 12 unvaccinated mice were challenged with influenza by instilling 50 μ l PBS containing $10 \times LD_{50}$ of mouse-adapted influenza A/Hong Kong/1/1968 (H3N2) into the nares of mice anesthetized with 2.5% isoflurane in oxygen. Mice were weighed and assessed for clinical score daily for 14 days. The clinical score consisted of 1 point for each of the following criteria: hunched posture, piloerection, abnormal gait, labored breathing, lethargy, and emaciation ($\geq 10\%$ body weight loss) (37). A subset of 4 mice from each group was sacrificed on day 4 and lungs were assessed for lung viral load by plaque assay (described in next section).

For the H1N1 experiment, groups of six female BALB/c mice from Charles River (Wilmington, MA) were vaccinated, i.n. or i.m., as described above, with 50 μ l of CoPoP/PHAD liposomes containing 100 ng his-tagged H1 HA from A/Hawaii/70/2019pdm (H1N1) or his-tagged H1 HA from A/California/04/2009pdm (H1N1) on day 0 and day 21. On day 42, the mice were challenged with influenza virus by instilling 50 μ l PBS containing $10 \times LD_{50}$ of mouse-adapted influenza A/California/04/2009pdm (H1N1) into the nares of mice anesthetized with 2.5% isoflurane in oxygen. Mice were weighed and assessed for clinical score daily for 14 days. Data for body weight changes, clinical score, and survival data were analyzed using Prism (GraphPad Software, San Diego, CA).

Influenza virus plaque assay in MDCK cells. MDCK cells (ATCC) were grown to 70% to 80% confluence in DMEM + 0.1 mM nonessential amino acids + 1 mM sodium pyruvate + 50 U/ml penicillin and 50 μ g/ml streptomycin + 20 μ g/ml gentamicin + 10% fcs in 6-well tissue culture plates in $37^\circ\text{C} + 5\% \text{CO}_2$. The medium was removed, the cells rinsed twice with 0.3% BSA in DMEM, and then 100 μ l 10-fold serial dilutions (0.3% BSA in DMEM as diluent) of virus samples were adsorbed for 1 h at $37^\circ\text{C} + 5\% \text{CO}_2$ (300 μ l diluent was added to each well during the adsorption to prevent drying of cell sheet). The inoculum was removed, and the cells rinsed once with PBS and then overlaid with 2 ml L-15 medium + 1 μ g/ml TPCK-treated trypsin + 0.5% agarose. The plates were incubated for 48 h and then stained with 0.3% crystal violet + 5% isopropanol + 5% ethanol in distilled water for 20 min following removal of the overlay and 30-min fixation in 90% ethanol. The cells were rinsed with distilled water, and the plaques were enumerated.

Serology. Collected blood from mice was centrifuged 15 min at 2,000 rcf, and separated serum was collected and stored at 4°C . ELISA was performed on serum samples; dilutions were prepared using 0.05% Tween20 in PBS (PBST) following either 2-fold or 10-fold serial dilutions. Plates were coated with HA antigen trimers or six-histidine peptide (Genscript; catalog no. RP11737; Fig. S2) in a coating buffer (5.3 g/liter Na_2CO_3 and 4.2 g/liter NaHCO_3 in deionized water, pH 9.6) at 1 μ g/ml and incubated overnight at 4°C . Plates were washed three times with PBST and incubated in 2% BSA in PBST for 2 h at 37°C with constant shaking. Dilutions were prepared during this incubation period and transferred to coated plates, then incubated again for 1 h at 37°C . Plates were washed three times with PBST and 100 μ l of 1 mg/liter goat anti-mouse secondary antibody with horseradish peroxidase (Goat Anti-Mouse IgG Antibody [H&L] [HRP]; GenScript; catalog no. A00160) was applied, followed by another 30-min incubation at 37°C . Plates were then washed six times with PBST, and 100 μ l 3,3',5,5'-tetramethylbenzidine (TMB) solution (TMB One Component Microwell Substrate; SouthernBiotech; catalog no. 0410-01) was added and developed for 5 min. The addition of 100 μ l of 1 M HCl was used to stop the reaction, and absorbance was read at 450 nm using a Tecan Safire microplate reader. Titers were defined as the reciprocal of the highest sera dilution producing an absorbance of greater than 0.5.

Nasal lavage. Mice were anesthetized with 2.5% isoflurane in oxygen, sacrificed by exsanguination, and then decapitated. A 0.3-cc syringe was used to pass sterile saline through the nasal passages via the trachea, with fluid collected in a 2-ml microcentrifuge tube placed under the nostrils. Each nasal passage was washed three times to collect a total volume of 1,800 μ l fluid per mouse, which was aliquoted and stored at -80°C .

Lung homogenization. Excised lungs from sacrificed mice were placed within a 1.5-ml tube containing 500 μ l Roswell Park Memorial Institute (RPMI) medium with 3 mg/ml collagenase enzyme and metallic oxide beads. Sample tubes were placed in a Bullet Blender Storm homogenizer (Next Advance, Troy, NY) for 15 min, speed setting 12. Samples were then incubated at 37°C for 1 h with constant shaking. Following incubation, samples were centrifuged for 15 min at 1,000 rcf, and liquid supernatant was extracted from the homogenized lung tissue.

Cryo-transmission electron microscopy characterization. Samples analyzed by cryo-TEM were vitrified using a Vitrobot Mark IV (Thermo Fisher Scientific). To increase the concentration of liposomes inside the holes in the grids, samples were applied twice to the grids. In the first application, a volume of 3.6 μ l was applied to the holey carbon grids and manually blotted using the Vitrobot blotting paper (Standard

Vitrobot Filter Paper, Ø55/20 mm, Grade 595). Right after blotting, a new drop of the sample was applied to the EM grid and blotted again using the standard routine with the two blotting pads in the Vitrobot Mark IV for 3 sec and with a blot force +1 before they were plunged into liquid ethane. The Vitrobot was set at 25°C and 100% relative humidity. The grids used for these experiments were C-flat 2/2-2Cu-T, and before the samples were applied, they were washed with chloroform for 2 h and treated with negative glow discharge in air at 5 mA for 15 s.

Vitrified grids were imaged in a Tecnai F20 electron microscope operated at 200 kV. Grids were loaded into the instrument using a Gatan 626 single tilt cryoholder. Images were collected at a magnification of 50,000 \times , which produced images with a calibrated pixel size of 2.145 Å. Images were collected with a total dose of $\sim 50 \text{ e}^-/\text{Å}^2$ using a defocus ranging from $-2 \mu\text{m}$ to $-2.50 \mu\text{m}$. Images were cropped and prepared for the figures using Adobe Photoshop.

Ethics. Experimental protocols involving mice, including immunizations and subsequent challenge studies, were reviewed and approved by the University at Buffalo, Veterans Administration Western New York Healthcare System (VAWNYHS), and University of Rochester Institutional Animal Care and Use Committees.

SUPPLEMENTAL MATERIAL

Supplemental material is available online only.

SUPPLEMENTAL FILE 1, PDF file, 0.1 MB.

ACKNOWLEDGMENTS

We acknowledge James Steven for valuable discussion. We thank staff members of the Parrish Facility for Electron Microscopy Research (FEMR) at McGill University for help in microscope operation and data collection. We also thank Collins of the Baker Institute for Animal Health at Cornell providing the influenza A/Ca/Illinois/41915/2015 (H3N2), as well as Richard J. Webby of Saint Jude Children's Research Hospital (Memphis, TN) for supplying the mouse-adapted influenza A/California/04/2009pdm (H1N1).

FEMR is supported by the Canadian Foundation for Innovation, the Quebec government, and McGill University. This research was partially funded by the New York Influenza Center of Excellence (NYICE), a member of the National Institute of Allergy Infectious Diseases (NIAID), National Institutes of Health (NIH), Department of Health and Human Services, Centers of Excellence for Influenza Research and Surveillance (CEIRS) contract no. HHSN272201400005C (NYICE), and NIH/NIAID 1R01AI145332 and R01AI141607 to L.M.-S., as well as 1R41AI149954 and 5R01HL151498 to B.A.D. This material is the result of work supported with resources and the use of facilities at the Veterans Administration Western New York Healthcare System, Buffalo, NY. The contents of this manuscript do not represent the views of the Department of Veterans Affairs or the United States Government.

J.F.L. and W.-C.H. hold competing interests in POP Biotechnologies. Other authors declare no competing interests.

REFERENCES

- Centers for Disease Control and Prevention. 2022. CDC seasonal flu vaccine effectiveness studies. <https://www.cdc.gov/flu/vaccines-work/effectiveness-studies.htm>. Accessed 3 August 2022.
- Centers for Disease Control and Prevention. 2021. Flu vaccination coverage, United States, 2020–2021 influenza season. <https://www.cdc.gov/flu/fluview/coverage-2021estimates.htm>. Accessed 7 October 2021.
- Tumpney TM, Renshaw M, Clements JD, Katz JM. 2001. Mucosal delivery of inactivated influenza vaccine induces B-cell-dependent heterosubtypic cross-protection against lethal influenza A H5N1 virus infection. *J Virol* 75:5141–5150. <https://doi.org/10.1128/JVI.75.11.5141-5150.2001>.
- Sendi P, Locher R, Bucheli B, Battegay M. 2004. Intranasal influenza vaccine in a working population. *Clin Infect Dis* 38:974–980. <https://doi.org/10.1086/386330>.
- Kiderman A, Furst A, Stewart B, Greenbaum E, Morag A, Zakay-Rones Z. 2001. A double-blind trial of a new inactivated, trivalent, intra-nasal anti-influenza vaccine in general practice: relationship between immunogenicity and respiratory morbidity over the winter of 1997–98. *J Clin Virol* 20:155–161. [https://doi.org/10.1016/S1386-6532\(00\)00175-X](https://doi.org/10.1016/S1386-6532(00)00175-X).
- Muszkat M, Yehuda AB, Schein MH, Friedlander Y, Naveh P, Greenbaum E, Schlesinger M, Levy R, Zakay-Rones Z, Friedman G. 2000. Local and systemic immune response in community-dwelling elderly after intranasal or intramuscular immunization with inactivated influenza vaccine. *J Med Virol* 61:100–106. [https://doi.org/10.1002/\(SICI\)1096-9071\(200005\)61:1%3C100::AID-JMV16%3E3.0.CO;2-5](https://doi.org/10.1002/(SICI)1096-9071(200005)61:1%3C100::AID-JMV16%3E3.0.CO;2-5).
- Glück U, Gebbers JO, Glück R. 1999. Phase 1 evaluation of intranasal virosomal influenza vaccine with and without *Escherichia coli* heat-labile toxin in adult volunteers. *J Virol* 73:7780–7786. <https://doi.org/10.1128/JVI.73.9.7780-7786.1999>.
- Holmgren J, Czerkinsky C. 2005. Mucosal immunity and vaccines. *Nat Med* 11: S45–S53. <https://doi.org/10.1038/nm1213>.
- Hasegawa H, Ichinohe T, Aina A, Tamura S-I, Kurata T. 2009. Development of mucosal adjuvants for intranasal vaccine for H5N1 influenza viruses. *Ther Clin Risk Manag* 5:125–132. <https://doi.org/10.2147/tcrm.s3297>.
- van Riet E, Aina A, Suzuki T, Hasegawa H. 2012. Mucosal IgA responses in influenza virus infections; thoughts for vaccine design. *Vaccine* 30:5893–5900. <https://doi.org/10.1016/j.vaccine.2012.04.109>.
- Lycke N. 2012. Recent progress in mucosal vaccine development: potential and limitations. *Nat Rev Immunol* 12:592–605. <https://doi.org/10.1038/nri3251>.
- Carter NJ, Curran MP. 2011. Live attenuated influenza vaccine (FluMist; FluenzTM). *Drugs* 71:1591–1622. <https://doi.org/10.2165/11206860-000000000-00000>.
- Dibben O, Crowe J, Cooper S, Hill L, Schewe KE, Bright H. 2021. Defining the root cause of reduced H1N1 live attenuated influenza vaccine effectiveness: low viral fitness leads to inter-strain competition. *NPJ Vaccines* 6:1–12. <https://doi.org/10.1038/s41541-020-00265-5>.
- Wang S, Liu H, Zhang X, Qian F. 2015. Intranasal and oral vaccination with protein-based antigens: advantages, challenges and formulation strategies. *Protein Cell* 6:480–503. <https://doi.org/10.1007/s13238-015-0164-2>.

15. Durrer P, Glück U, Spyr C, Lang AB, Zurbriggen R, Herzog C, Glück R. 2003. Mucosal antibody response induced with a nasal virosome-based influenza vaccine. *Vaccine* 21:4328–4334. [https://doi.org/10.1016/s0264-410x\(03\)00457-2](https://doi.org/10.1016/s0264-410x(03)00457-2).
16. Christensen D, Foged C, Rosenkrands I, Lundberg CV, Andersen P, Agger EM, Nielsen HM. 2010. CAF01 liposomes as a mucosal vaccine adjuvant: in vitro and in vivo investigations. *Int J Pharm* 390:19–24. <https://doi.org/10.1016/j.ijpharm.2009.10.043>.
17. Dong C, Wang Y, Gonzalez GX, Ma Y, Song Y, Wang S, Kang S-M, Compans RW, Wang B-Z. 2021. Intranasal vaccination with influenza HA/GO-PEI nanoparticles provides immune protection against homo- and heterologous strains. *Proc Natl Acad Sci U S A* 118:e2024998118. <https://doi.org/10.1073/pnas.2024998118>.
18. Sia ZR, He X, Zhang A, Ang JC, Shao S, Seffouh A, Huang WC, D'Agostino MR, Teimouri Dereshgi A, Suryaprakash S, Ortega J, Andersen H, Miller MS, Davidson BA, Lovell JF. 2021. A liposome-displayed hemagglutinin vaccine platform protects mice and ferrets from heterologous influenza virus challenge. *Proc Natl Acad Sci U S A* 118:e2025759118. <https://doi.org/10.1073/pnas.2025759118>.
19. Shao S, Geng J, Ah Yi H, Gogia S, Neelamegham S, Jacobs A, Lovell JF. 2015. Functionalization of cobalt porphyrin-phospholipid bilayers with his-tagged ligands and antigens. *Nat Chem* 7:438–446. <https://doi.org/10.1038/nchem.2236>.
20. Carter KA, Shao S, Hoopes MI, Luo D, Ahsan B, Grigoryants VM, Song W, Huang H, Zhang G, Pandey RK, Geng J, Pfeifer BA, Scholes CP, Ortega J, Karttunen M, Lovell JF. 2014. Porphyrin-phospholipid liposomes permeabilized by near-infrared light. *Nat Commun* 5:3546. <https://doi.org/10.1038/ncomms4546>.
21. Nogales A, Huang K, Chauché C, DeDiego ML, Murcia PR, Parrish CR, Martínez-Sobrido L. 2017. Canine influenza viruses with modified NS1 proteins for the development of live-attenuated vaccines. *Virology* 500:1–10. <https://doi.org/10.1016/j.virol.2016.10.008>.
22. Cao L, Lou J, Zhao S, Chan RWY, Chan M, Wu WKK, Chong MKC, Zee BC-Y, Yeoh EK, Wong SY-S, Chan PKS, Wang MH. 2021. In silico prediction of influenza vaccine effectiveness by sequence analysis. *Vaccine* 39:1030–1034. <https://doi.org/10.1016/j.vaccine.2021.01.006>.
23. Huang W-C, Deng B, Lin C, Carter KA, Geng J, Razi A, He X, Chitgupi U, Federizon J, Sun B, Long CA, Ortega J, Dutta S, King CR, Miura K, Lee S-M, Lovell JF. 2018. A malaria vaccine adjuvant based on recombinant antigen binding to liposomes. *Nat Nanotechnol* 13:1174–1181. <https://doi.org/10.1038/s41565-018-0271-3>.
24. Halsey NA, Talaat KR, Greenbaum A, Mensah E, Dudley MZ, Proveaux T, Salmon DA. 2015. The safety of influenza vaccines in children: an Institute for Vaccine Safety white paper. *Vaccine* 33(Suppl 5):F1–F67. <https://doi.org/10.1016/j.vaccine.2015.10.080>.
25. Mutsch M, Zhou W, Rhodes P, Bopp M, Chen RT, Linder T, Spyr C, Steffen R. 2004. Use of the inactivated intranasal influenza vaccine and the risk of Bell's palsy in Switzerland. *N Engl J Med* 350:896–903. <https://doi.org/10.1056/NEJMoa030595>.
26. Ribeiro RS, Ferreira IM, Figueiredo I, Jr, Vericimo MA. 2015. Access to the tracheal pulmonary pathway in small rodents. *J Brasil Patol Med Lab* 51:183–188. <https://doi.org/10.5935/1676-2444.20150032>.
27. Helmy SAK, Al-Attayah RJ. 2000. The effect of halothane and isoflurane on plasma cytokine levels. *Anaesthesia* 55:904–910. <https://doi.org/10.1046/j.1365-2044.2000.01472-2.x>.
28. Huang W-C, Mabrouk MT, Zhou L, Baba M, Tachibana M, Torii M, Takashima E, Locke E, Plieskatt J, King CR, Coelho CH, Duffy PE, Long C, Tsuboi T, Miura K, Wu Y, Ishino T, Lovell JF. 2022. Vaccine co-display of CSP and Pfs230 on liposomes targeting two *Plasmodium falciparum* differentiation stages. *Commun Biol* 5:773. <https://doi.org/10.1038/s42003-022-03688-z>.
29. Mabrouk MT, Huang W-C, Deng B, Li-Purcell N, Seffouh A, Ortega J, Ekin Atilla-Gokcumen G, Long CA, Miura K, Lovell JF. 2020. Lyophilized, antigen-bound liposomes with reduced MPLA and enhanced thermostability. *Int J Pharm* 589:119843. <https://doi.org/10.1016/j.ijpharm.2020.119843>.
30. Huang W-C, Zhou S, He X, Chiem K, Mabrouk MT, Nissly RH, Bird IM, Strauss M, Sambhara S, Ortega J, Wohlfert EA, Martínez-Sobrido L, Kuchipudi SV, Davidson BA, Lovell JF. 2020. SARS-CoV-2 RBD neutralizing antibody induction is enhanced by particulate vaccination. *Adv Mater* 32:e2005637. <https://doi.org/10.1002/adma.202005637>.
31. Federizon J, Frye A, Huang W-C, Hart TM, He X, Beltran C, Marcinkiewicz AL, Mainprize IL, Wills MKB, Lin Y-P, Lovell JF. 2020. Immunogenicity of the Lyme disease antigen OspA, particleized by cobalt porphyrin-phospholipid liposomes. *Vaccine* 38:942–950. <https://doi.org/10.1016/j.vaccine.2019.10.073>.
32. Mabrouk MT, Chiem K, Rujas E, Huang W-C, Jahagirdar D, Quinn B, Surendran Nair M, Nissly RH, Cavener VS, Boyle NR, Sornberger TA, Kuchipudi SV, Ortega J, Julien J-P, Martínez-Sobrido L, Lovell J. 2021. Lyophilized, thermostable Spike or RBD immunogenic liposomes induce protective immunity against SARS-CoV-2 in mice. *Sci Adv* 7:eabj1476. <https://doi.org/10.1126/sciadv.abj1476>.
33. He X, Zhou S, Quinn B, Jahagirdar D, Ortega J, Abrams SI, Lovell JF. 2021. HPV-associated tumor eradication by vaccination with synthetic short peptides and particle-forming liposomes. *Small* 17:e2007165. <https://doi.org/10.1002/sml.202007165>.
34. Quan F-S, Compans RW, Nguyen HH, Kang S-M. 2008. Induction of hetero-subtypic immunity to influenza virus by intranasal immunization. *J Virol* 82:1350–1359. <https://doi.org/10.1128/JVI.01615-07>.
35. De Filette M, Fiers W, Martens W, Birkett A, Ramne A, Löwenadler B, Lycke N, Jou WM, Saelens X. 2006. Improved design and intranasal delivery of an M2e-based human influenza A vaccine. *Vaccine* 24:6597–6601. <https://doi.org/10.1016/j.vaccine.2006.05.082>.
36. Huang W-C, Deng B, Mabrouk MT, Seffouh A, Ortega J, Long C, Miura K, Wu Y, Lovell JF. 2020. Particle-based, Pfs230 and Pfs25 immunization is effective, but not improved by duplexing at fixed total antigen dose. *Malar J* 19:309. <https://doi.org/10.1186/s12936-020-03368-5>.
37. Bonville CA, Bennett NJ, Koehnlein M, Haines DM, Ellis JA, DeVecchio AM, Rosenberg HF, Domachowske JB. 2006. Respiratory dysfunction and proinflammatory chemokines in the pneumonia virus of mice (PVM) model of viral bronchiolitis. *Virology* 349:87–95. <https://doi.org/10.1016/j.virol.2006.02.017>.